SPE-166850-PP

Improved Geomagnetic Referencing in the Arctic Environment

Benny Poedjono and Nathan Beck, SPE, Schlumberger; Andrew Buchanan, SPE, and Luca Borri, Eni Petroleum Co.; Stefan Maus, SPE, Magnetic Variation Services; and Carol A. Finn, E. William Worthington and Tim White, US Geological Survey

This paper was prepared for presentation at the SPE Arctic and Extreme Environments Conference & Exhibition held in Moscow, Russia, 15–17 October 2013.

Abstract

Geomagnetic referencing uses the Earth's magnetic field to determine accurate wellbore positioning essential for success in today's complex drilling programs, either as an alternative or a complement to north-seeking gyroscopic referencing. However, fluctuations in the geomagnetic field, especially at high latitudes, make the application of geomagnetic referencing in those areas more challenging. Precise crustal mapping and the monitoring of real-time variations by nearby magnetic observatories is crucial to achieving the required geomagnetic referencing accuracy. The Deadhorse Magnetic Observatory (DED), located at Prudhoe Bay, Alaska, has already played a vital role in the success of several commercial ventures in the area, providing essential, accurate, real-time data to the oilfield drilling industry. Geomagnetic referencing is enhanced with real-time data from DED and other observatories, and has been successfully used for accurate wellbore positioning. The availability of real-time geomagnetic measurements leads to significant cost and time savings in wellbore surveying, improving accuracy and alleviating the need for more expensive surveying techniques. The correct implementation of geomagnetic referencing is particularly critical as we approach the increased activity associated with the upcoming maximum of the 11-year solar cycle. The DED observatory further provides an important service to scientific communities engaged in studies of ionospheric, magnetospheric and space weather phenomena.

Introduction

Drilling along the North coast of Alaska poses a number of challenges that demand an advanced approach to wellbore surveying. Due to both the crowded subterranean environment and the geological complexity of the onshore North Slope of Alaska and the offshore Beaufort Sea **(Fig. 1)**, precise, real-time wellbore positioning is essential to the success of commercial development.

First and foremost, the prevention of accidental intersections with adjacent wellbores is critical due to the associated Health, Safety and Environmental (HSE) risk as well as minimizing the non-HSE risks. By implementing highly accurate surveys, the ellipses of uncertainty (EOUs) will be minimized. By avoiding the overlapping of EOUs that could occur with conventional measurement-while-drilling (MWD) surveys, the probability of a wellbore collision can be greatly diminished. The complexity of the targeted reservoirs provides another critical impetus for higher surveying accuracy. Accurate well placement is critical to optimize or avoid fault crossings and to maximize reservoir drainage. It is vital that wellbores are placed with adequate accuracy to ensure proper spacing between injector and producer wells.

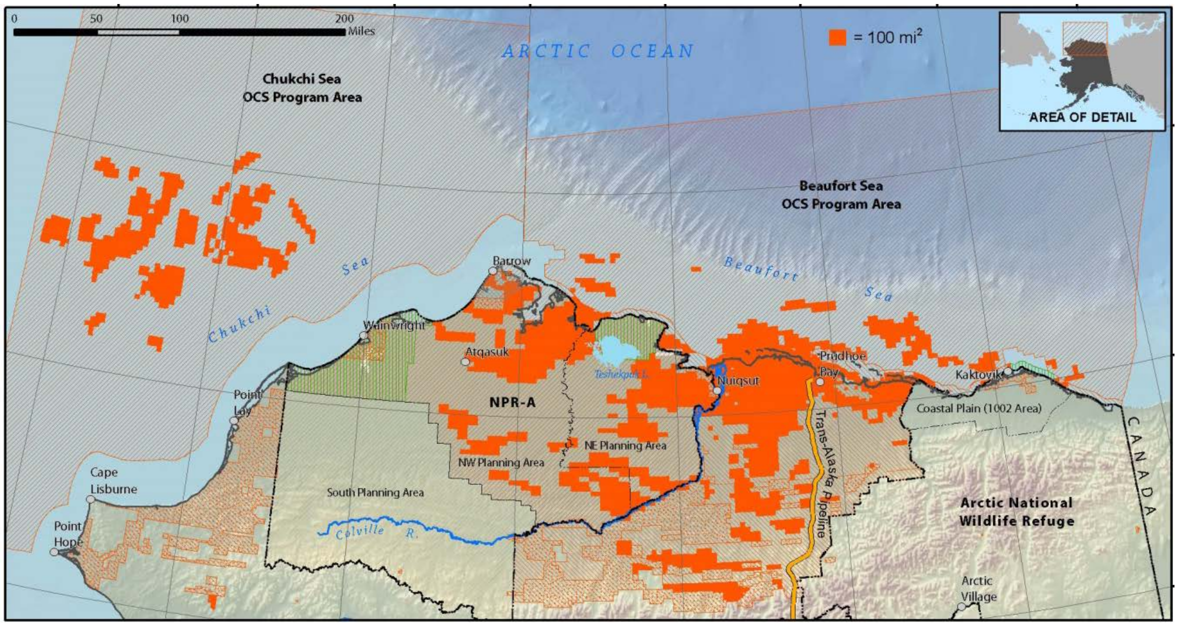

Fig. 1–Map of the North Slope of Alaska and offshore Beaufort Sea. Sold Federal and State leases shown in orange and active state leases in shaded orange.

Why Geomagnetic Referencing is Needed

As noted above, accurate wellbore positioning is essential to locate and produce the resources in the Arctic. Unfortunately, the high latitudes associated with Arctic drilling pose a challenge to standard magnetic surveying techniques. Most notably, the accuracy of standard MWD survey can be compromised at high latitude because of smaller horizontal magnetic field values. High inclination limitations and the extensive time requirements of implementing traditional gyroscopic surveys limit their effectiveness. An accurate and efficient solution is required to the success of drilling in the Arctic environments.

Geomagnetic referencing provides this solution by simultaneously addressing the stringent well placement requirements and the challenging surveying environment of Alaskan North Slope operations. Precise real-time positioning is possible by taking advantage of refinements in the latest developments in crustal model processing and improvements in the magnetic observatory design that measure disturbance fields **(Fig. 2)**. As such, geomagnetic referencing techniques have been deemed capable of addressing the challenges to survey accuracy inherent in high-latitude drilling, particularly in areas dealing with high-disturbance components of Earth's magnetic field as well as the need to compensate for the effect of drillstring interference.

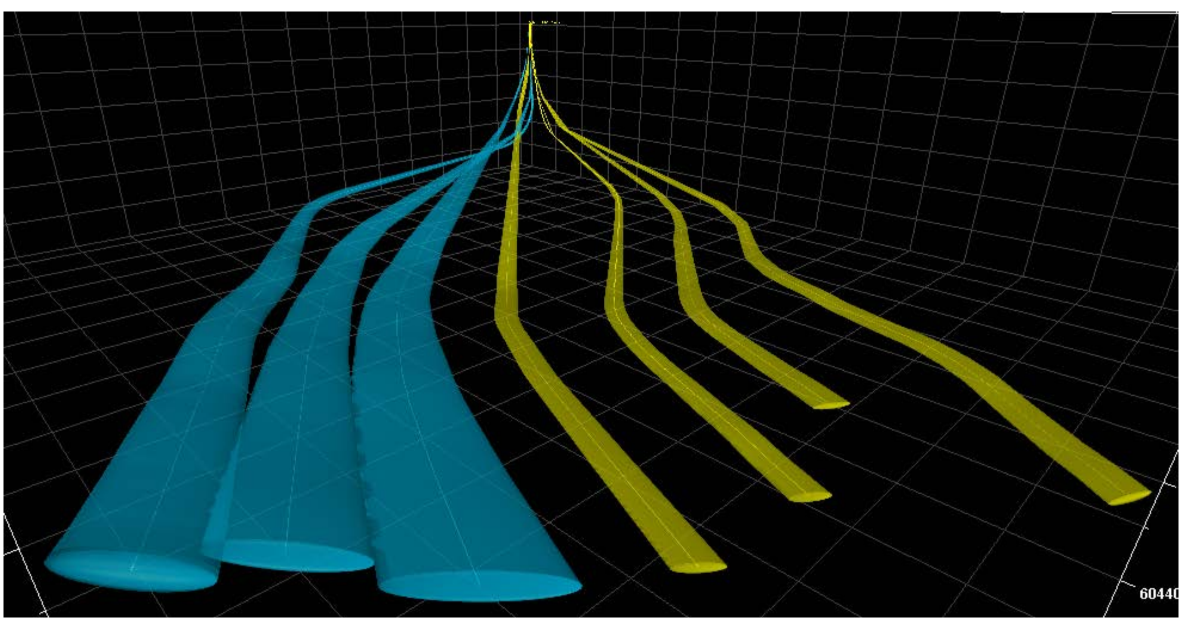

Fig. 2 - The difference in ellipses of uncertainty (EOUs) between the measurement while drilling (in blue) and geomagnetic referencing (in yellow).

Geomagnetic Referencing at High Latitudes

Directional drilling requires accurate knowledge of the orientation of bottom-hole assembly (BHA) referenced to vertical (inclination) and to true north (azimuth). To acquire these critical measurements, wellbore surveying by MWD uses the direction of Earth's gravity and magnetic field as a natural reference frame. Specifically, the horizontal component of the geomagnetic field is the key reference when using magnetic north to determine azimuthal orientation of the borehole. At higher latitudes, the strength of the horizontal component of the geomagnetic field shrinks, which exacerbates any error sources that accumulate while surveying.

Based on the smaller horizontal geomagnetic component, there is an increased impact from axial and cross-axial interference from the drillstring and/or mud effects. BHAs that are magnetically acceptable in lower latitude areas can lead to significant inaccuracies in the Arctic environments.

The geomagnetic field can be divided into three contributions:

- The **main field** generated by the geodynamo in the Earth's core. For practical purposes, the main field is defined as the internal field of spherical harmonic degree 1-15, excluding time varying fields with periods shorter than about 2 years **(Fig. 3)**.
- The **crustal field** caused by magnetic minerals in the crust. In practice, the crustal field is defined as the static internal field of spherical harmonic degree 16 and higher.
- **Magnetic disturbance fields** caused by electric currents in near-Earth space, and corresponding "mirror-currents" induced in the Earth and oceans.

Knowledge of the crustal field and real-time magnetic disturbance field is essential to provide an accurate wellbore position while drilling in the Arctic environments.

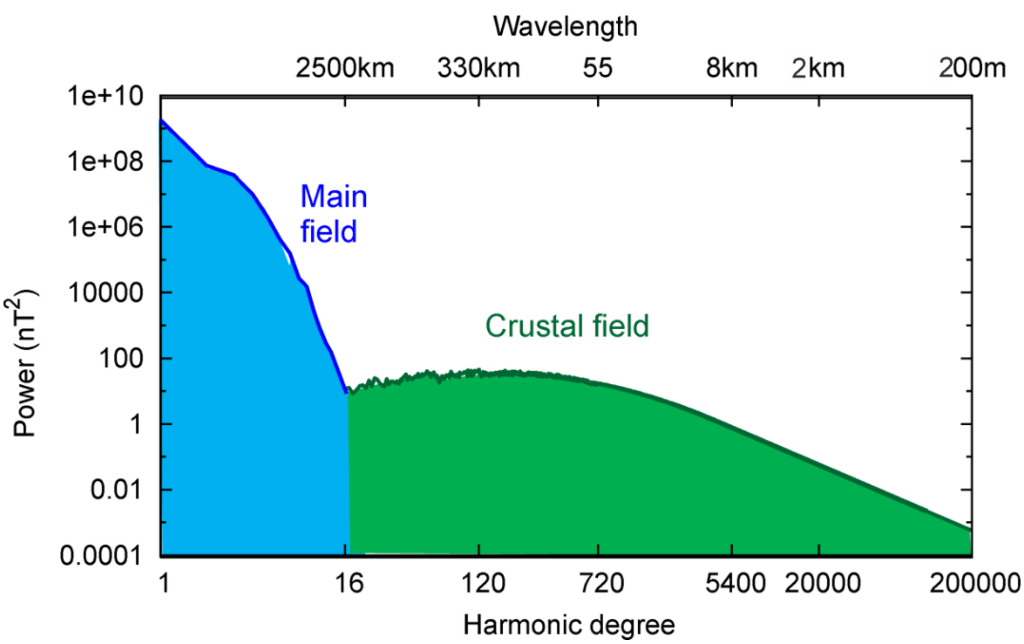

Fig. 3—Shows the main field (in blue) and crustal field (in green) contribution to the geomagnetic field.

Crustal Field Model

To accurately model the crustal magnetic field, it is important to consider its entire wavelength spectrum. Satellite observations cover the long wavelengths down to 250 km. The shorter wavelengths are best provided by local aeromagnetic surveys. The project area for this study is well covered by large-scale aeromagnetic surveys **(Fig. 4)**. Coverage of the drillsite and the southern onshore region by USGS aeromagnetic surveys (http://mrdata.usgs.gov/geophysics/surveys-ak.html) was extended to the north over the Arctic Ocean with surveys of the U. S. Naval Research Laboratory (NRL) which are publicly available at http://www.ngdc.noaa.gov/mgg/trk/aeromag/nrl_arctic/. Due to concerns about data reliability, emphasis is placed on quality control and validation. The NRL surveys in the Northern section show good agreement in their overlap with the USGS-165 aeromagnetic survey to the South **(Fig. 5)**.

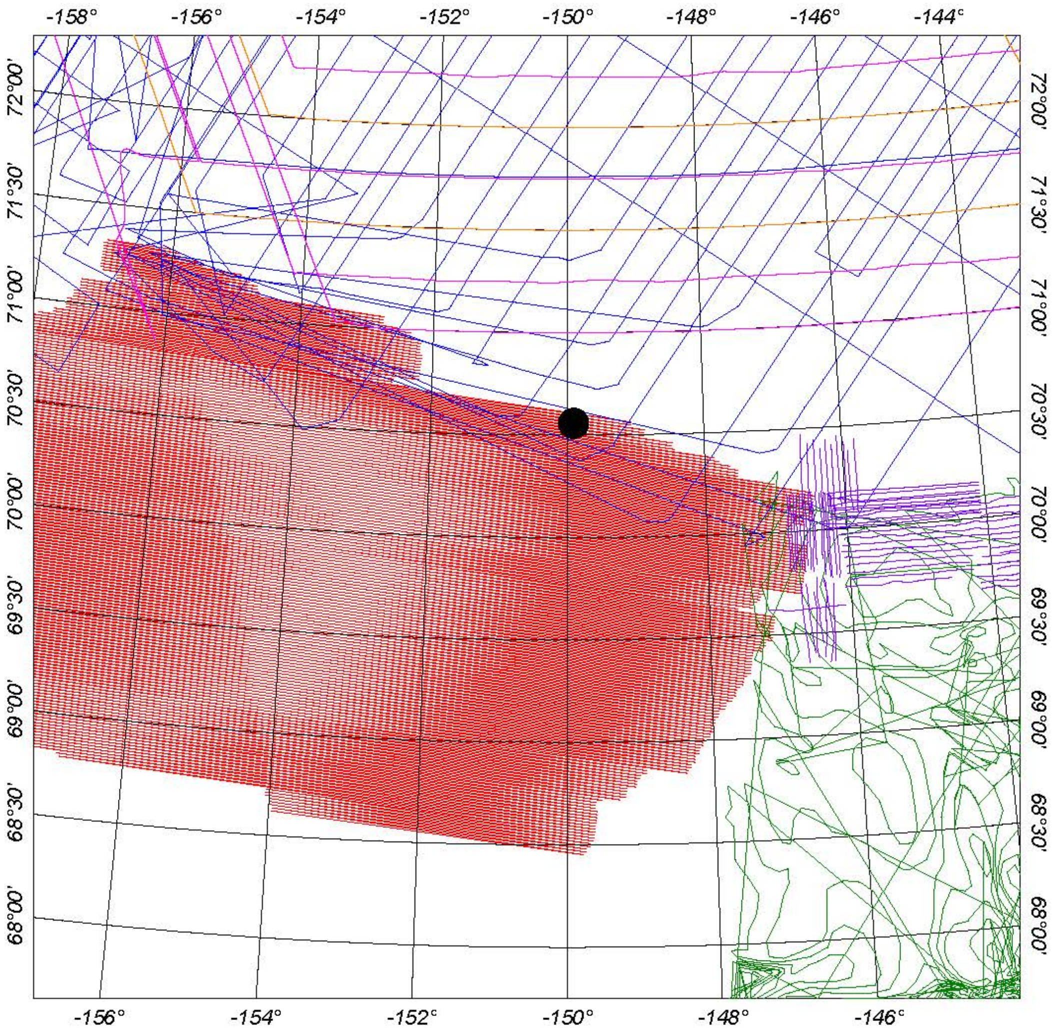

Fig. 4—Flight lines of the magnetic surveys used for this project, which are from Naval Research Laboratory (NRL) for the northern region and from the United States Geological Survey (USGS) for the southern region (red, purple and green). The black dot is the proposed drill location. The missing area to the Southwest was filled in from the USGS Alaska Aeromagnetic Compilation, which also includes the USGS-165, 550 and 21-22 surveys.

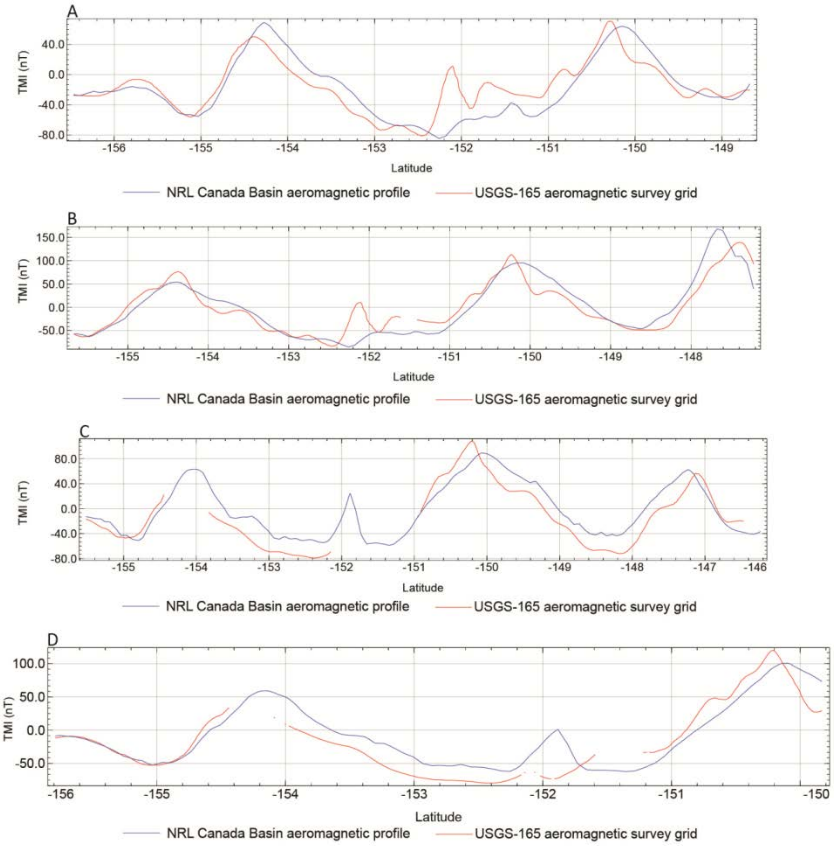

Fig. 5—The comparison of profiles shows that the USGS-165 survey has a slightly better resolution, showing more detail than the smoother NRL Canada Basin survey. The gaps in the USGS-165 (red line) indicate missing coverage in the USGS-165 survey. Agreement between the two surveys is fairly good for the long wavelengths, with overall root-mean-square deviations of about 20 nT.

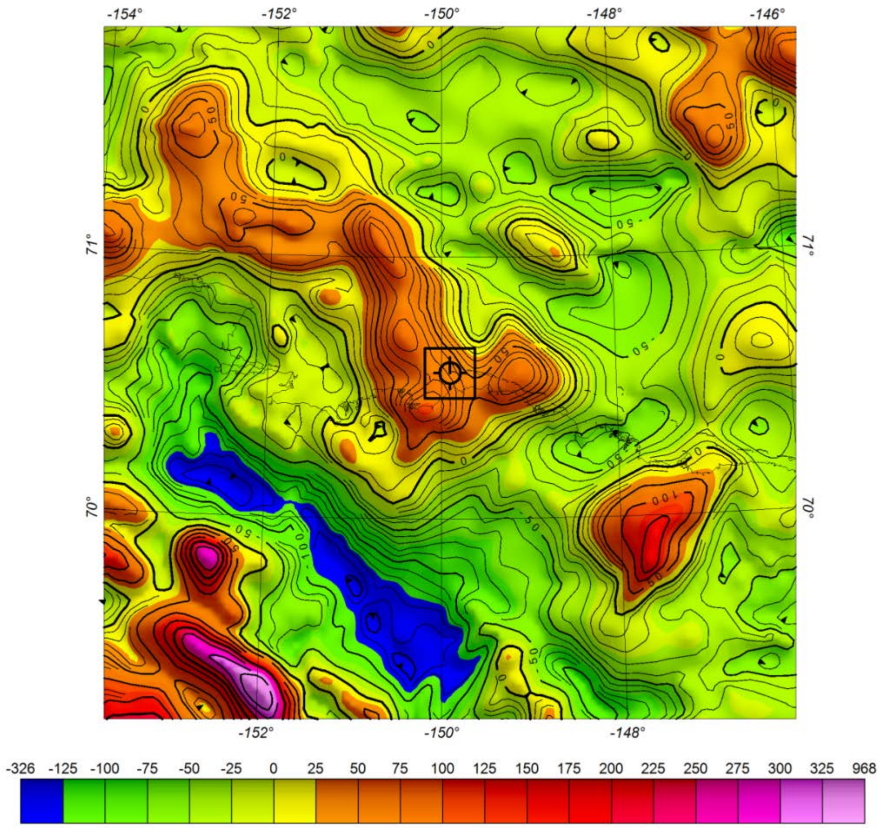

Fig. 6–Observed total field anomaly after all surveys in the area were merged, with lease area (black dot) and drillsite location (black cross hair).

After merging and validating, the input data are transformed into a 3D magnetic model for the lease area **(Fig. 6)**. The input data set only specifies the total intensity of the geomagnetic field, which can be thought of as the length of the magnetic field vector. Its direction has to be separately estimated by geomagnetic modeling. For a single location, the direction of the magnetic field cannot be inferred from the strength of the field alone. However, if the field is known in a sufficiently large area, the solution of Laplace's differential equation for that area provides an estimate of the full vector of the geomagnetic field. To solve Laplace's equation, the magnetic field vector is first represented as the negative gradient of a scalar magnetic potential (Maxwell's Equation in source-free region).

$$\mathbf{B} = -\nabla \mathbf{V}$$

The potential V is then expanded into harmonic functions. Since the Earth shape is best approximated by an ellipsoid of rotation, the method employs ellipsoidal harmonics to represent the magnetic potential. These functions are defined as

$$V(\lambda,\beta,u) = R\sum_{n=1}^{N}\sum_{m=0}^{n}\frac{Q_n^m\left(i\frac{u}{E}\right)}{Q_n^m\left(i\frac{b}{E}\right)}(g_n^m\cos m\lambda + h_n^m\sin m\lambda)P_n^m(\sin\beta)$$

where λ is longitude, β is reduced latitude, u is the semi-minor axis of the confocal ellipsoid at this location, R is the traditional geomagnetic reference radius, N is the degree of the expansion, $i = \sqrt{-1}$, and P_n^m and Q_n^m are fully normalized associated Legendre functions of the first and second kind, respectively. E and b are the focus and semi-major axis of the 1984 World Geodetic System (WGS84) reference ellipsoid. Finally, g_n^m and h_n^m are the ellipsoidal harmonic model coefficients of the expansion, estimated by least squares from the input data for the area. A detailed validation study of the algorithm was recently published by Poedjono et al (2012).

The maps in **Figs. 7-9** show the crustal residuals at sea level and at the maximum drilling depth of 11,000 ft below sea level. The black square in each map indicates the coverage of the referencing cubes and the black cross-hair indicates the drillsite location.

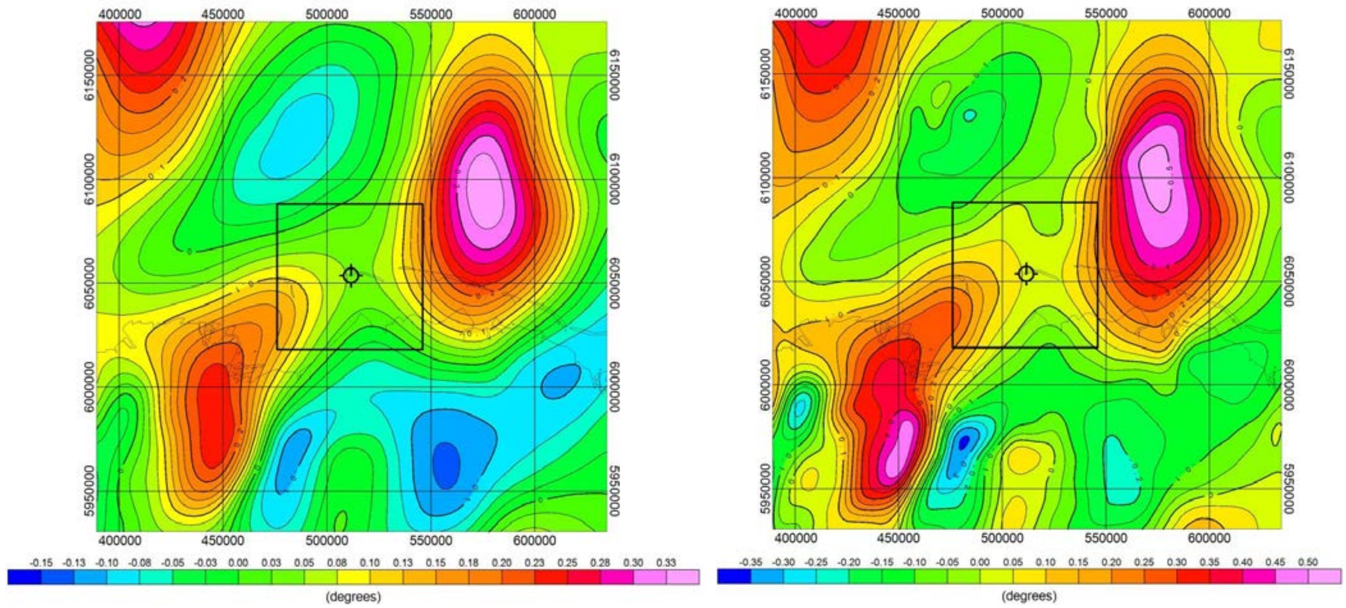

Fig. 7—The declination anomaly map at mean sea level (M.S.L.) and at maximum drilling depth of 11,000 ft True Vertical Depth (TVD). Coordinate eastings and northings are given in State Plane Coordinates, Alaska Zone 4, US Survey ft.

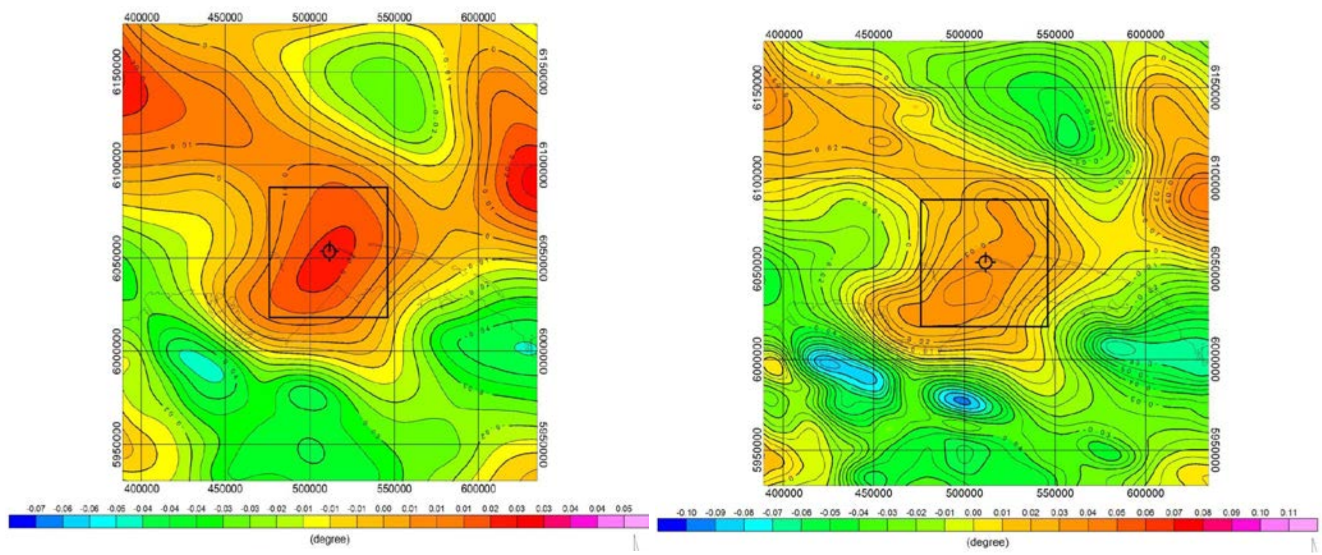

Fig. 8—The dip anomaly map at M.S.L. and at maximum drilling depth of 11,000 ft TVD. Coordinate eastings and northings are given in State Plane Coordinates, Alaska Zone 4, US Survey ft.

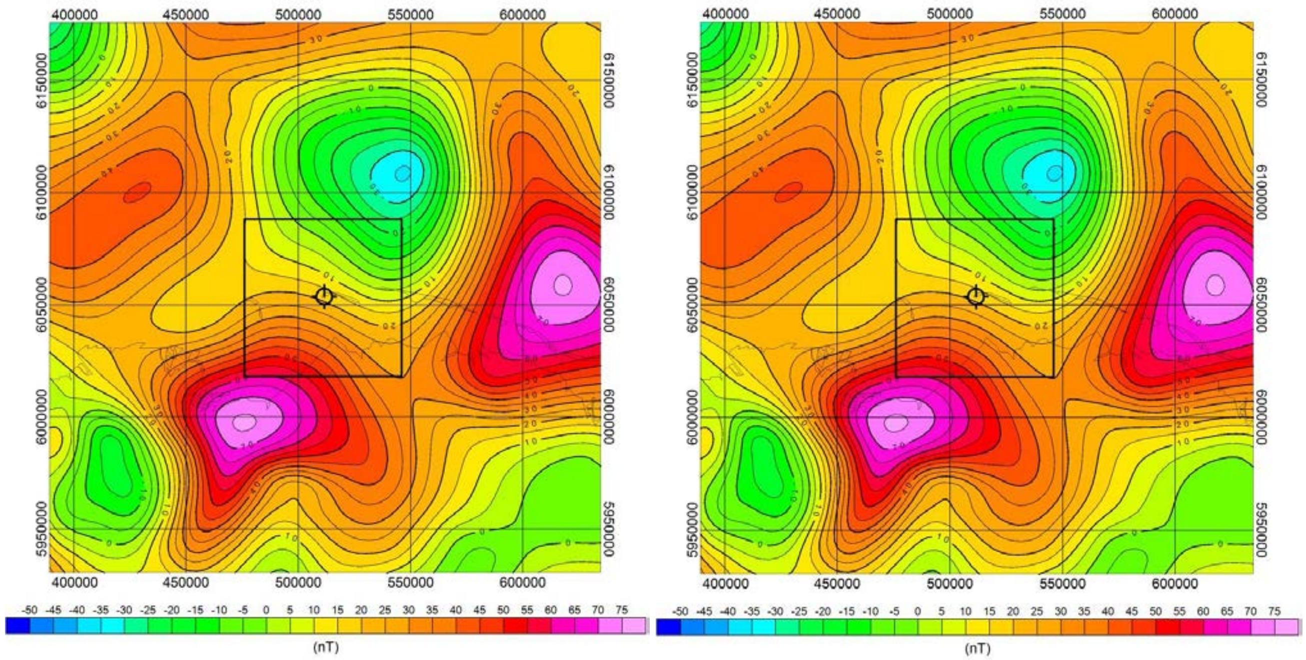

Fig. 9—The Total Magnetic Intensity (TMI) anomaly map at M.S.L. and at maximum drilling depth of 11,000 ft TVD. Coordinate eastings and northings are given in State Plane Coordinates, Alaska Zone 4, US Survey ft.

Disturbance Fields and the 11 Year Solar Sunspot Cycle

Disturbance fields strongly affect geomagnetic referencing at high latitudes for two reasons. First, the disturbance fields themselves are stronger here than at low latitudes. Second, the weaker horizontal intensity of the main field at high latitudes means that a horizontal disturbance of constant strength has a stronger affect on the declination here than at low latitudes.

The magnetic disturbance field in the Arctic is primarily due to electric currents in the magnetosphere and ionosphere. Secondary magnetic fields caused by electric currents induced in the oceans and solid Earth also play an important role. The magnetospheric current systems are fed by charged particles and magnetic fields ejected from the Sun. This solar wind is modulated by the 11-year sunspot cycle. The larger the number of sunspots, the higher the likelihood of coronal mass ejections and the stronger the solar wind. The Earth’s magnetic field acts as a shield against the solar wind, creating a cavity of about 20 Earth radii, which is called the magnetosphere.

The electric currents in the magnetosphere are coupled to currents in the ionosphere. This is a region of partially ionized gas about 80 km to 1000 km above the Earth’s surface. Currents in the ionosphere are present even during quiet times and are then caused by tides of the atmosphere. During magnetic storms, electric fields are imposed from the magnetosphere through field-aligned currents onto the polar ionosphere. These electric fields drive strong east-west currents called polar electrojets, which cause the largest magnetic disturbances at high latitudes. Cross-polar-cap ionospheric currents further contribute to the magnetic disturbances seen in the Arctic.

Time-varying magnetic fields further induce electric currents in the oceans and solid Earth. These make up roughly one-third of the observed magnetic disturbance field. The spatial structure of these induced currents can be quite complex because of the inhomogeneous conductivity of the Earth. This is why it is essential to have real-time magnetic measurements available in the vicinity of the drillsite.

Magnetic Observatory Data

The Deadhorse observatory was established in March 2010 at Prudhoe Bay, Alaska, in cooperation with the USGS, so that the data could be used for real-time corrections when using Geomagnetic Referencing (Poedjono et. al., 2012). In August 2012, the observatory was formally accepted as an Intermagnet Observatory (IMO), having demonstrated the high standards of data acquisition being obtained by the observatory. Certification of DED **(Fig. 10)** as an IMO also demonstrates the commitment to the highest quality magnetic field data possible, which is critical for practical real-time applications such as geomagnetic referencing. Data recorded at one-minute and one-second intervals are used, with the models described above, to compute the declination and dip angles at depth for use by the MWD tools.

In addition, data from the USGS observatories at Barrow and College, Alaska are also used. The Barrow magnetic observatory (BRW) is the northernmost point geographically in the U.S. The College Magnetic Observatory (CMO) is located in

Fairbanks, Alaska. The three observatories provide a somewhat unique visualization of the geomagnetic field and its behavior during magnetically active periods through their close geographic distribution. They also provide a relatively high level of spatial resolution, as can be seen in **Fig. 11**. The BRW and DED observatories are separated by about 300 km, primarily in the east/west direction. The CMO resides about 480 km south of BRW and DED. All three observatories are equipped with identical instrumentation and acquisition equipment. The instruments are low noise and high resolution and provide detailed recordings of active magnetic field data.

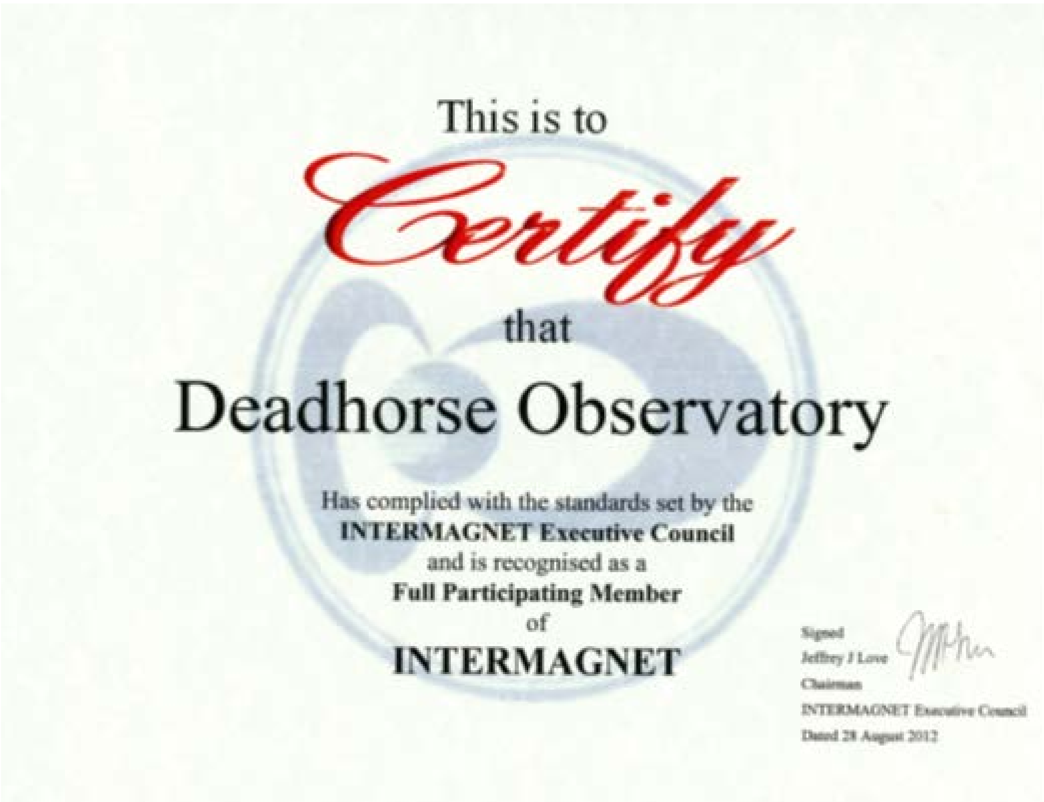
This is to
Certify
that
Deadhorse Observatory
Has complied with the standards set by the
INTERMAGNET Executive Council
and is recognised as a
Full Participating Member
of
INTERMAGNET

Signed
Jeffrey J Love
Chairman
INTERMAGNET Executive Council
Dated 28 August 2012

Fig. 10 — The DED INTERMAGNET certification.

Fig. 11—Location of DED relative to BRW and CMO

Characterization of the maximum magnetic disturbance field

To characterize the disturbance field, one-minute averaged measurements of the USGS magnetic observatories Barrow (BRW) and Deadhorse (DED) were used from 1995 to the present. In the first step, a spline was fitted to each magnetic field component at each observatory and was subtracted from the measurement. This procedure was used to remove the main and crustal field contribution, isolating the disturbance field. The residual Bx, By, and Bz values were then transformed into corresponding residuals of the declination, dip, and total field.

To derive time series of maximum disturbances, data analysis windows of three different lengths were moved over the residuals of both observatories to determine the running monthly maximum R_m, the running annual maximum R_y, and the running 4-year maximum R_{4y}. The final maximum was then computed as a weighted average of the maxima as

$$R = (3\,R_m + 2\,R_y + R_{4y}) / 6$$

This procedure was repeated separately for the declination, dip, and total field.

To model the disturbance and predict it outward, a Bezier spline was fitted to each of the time series of the maximum declination, dip and total field. After the end of 2012, the spline was then extrapolated outward, mirroring the curve for the previous solar cycle. **Fig. 12** shows the original time series (blue and red) and the fitted spline (solid black) from 1995 up to its extrapolation to 2020. To provide an envelope of the expected maximum and minimum disturbances, two additional dashed lines were drawn for 1.8*spline and spline/1.8. Based on **Fig. 12**, disturbance fields created significant changes in the declination from 2.5° to 20°; Dip from 0.7° to 4°; and total field from 300 nT to 1800 nT. Note that the maximum disturbance in the magnetic field lags the maximum of the solar activity cycle by about 2 years. Therefore, the maximum disturbance in the magnetic field during the current solar cycle is expected for 2015-2019, while the maximum of the solar sunspot cycle is expected to occur earlier.

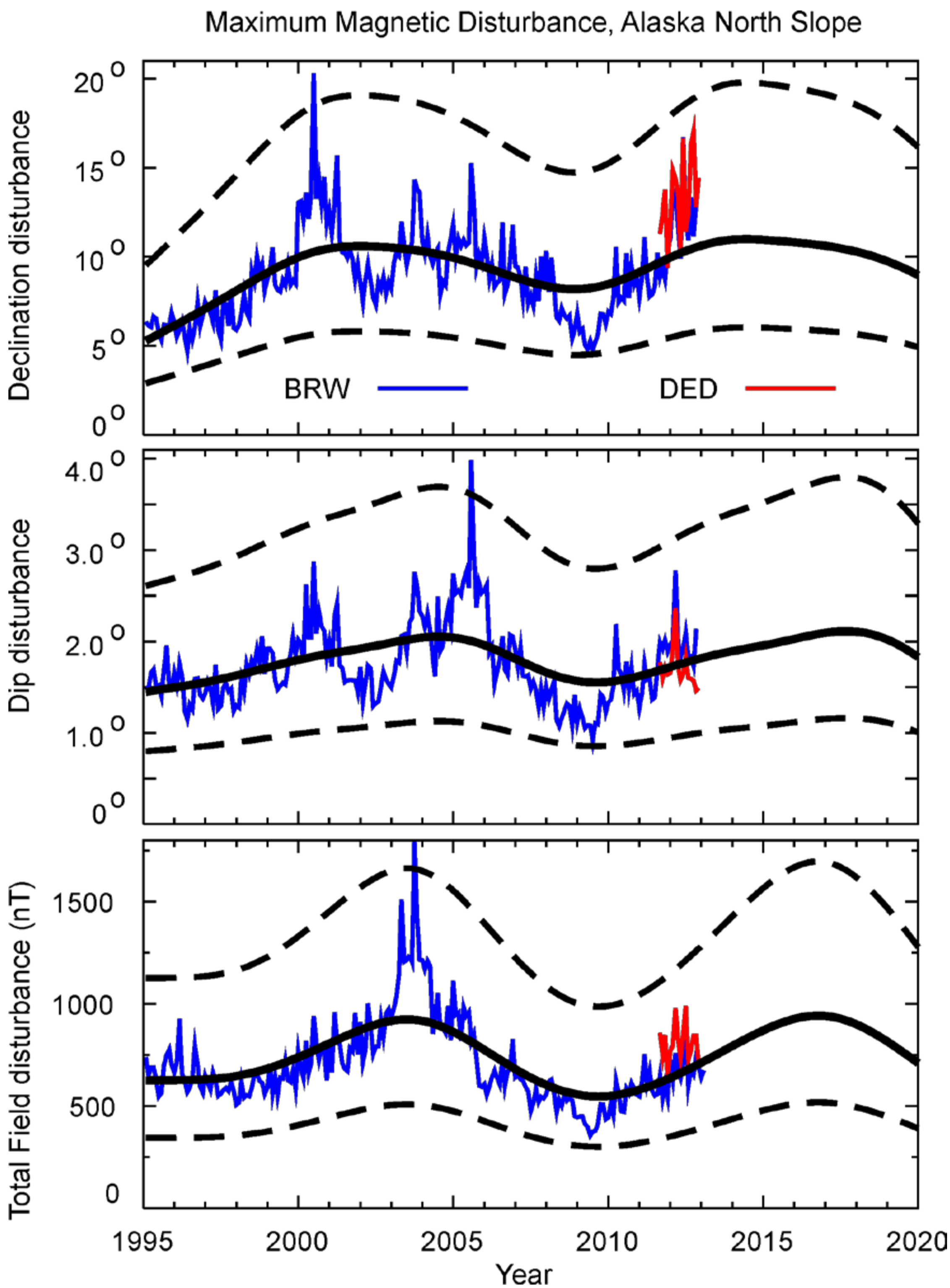

Fig. 12—Modulation of the maximum magnetic disturbances in Alaska with the 11 year solar sunspot cycle. The USGS Barrow observatory is shown in blue and the recently installed USGS Deadhorse observatory is shown in red.

A Closer Look at Declination During Magnetic Storms

On June 1, 2013, USGS reported a large magnetic storm. This event was classified by USGS to be in the 70th percentile in terms of the sudden commencement displacement – 30% of storms have a larger sudden commencement (Gannon 2012). USGS produces and publishes magnetic storm summaries for selected large events. The summary for this particular event is located at the following URL: http://geomag.usgs.gov/storm/17. Storms such as this one can occur several times per year, possibly more often during the solar maximum. This particular event was the focus of this study as we analyzed the differences between magnetic field measurements by the three USGS observatories: BRW, CMO and DED.

The data used in this analysis are the USGS raw one-second data product with minimal despiking applied. The instruments used to record these data are tri-axial Narod fluxgate magnetometers (Narod). The sensor has a core noise level of about 0.005 nT at 1 Hz. The resolution of the analog to digital converter is 24 bits, which when coupled with the Narod yields better than a 0.0001 nT resolution. However, data are reported to a 0.001 nT resolution, due to limitations in INTERMAGNET data formats. The sensor orientation used at the observatories is HEZ: During the initial installation of the instrument, the sensor is aligned using magnetic north as a reference. In this manner, most of the horizontal field is measured by the H axis of the sensor. This orientation allows for very sensitive measurements of the variation in declination.

The fluxgate sensors for the three observatories were installed at different times, which results in different reference frames for the raw data measured at these observatories. We cannot directly compare the raw data from each observatory until we rotate the data to the XYZ reference frame. For the XYZ reference frame, X is positive and oriented to geographic north, Y is positive geographic east and Z is positive down toward the Earth's core. Using these values we can compute the magnetic declination related to geographic north. Declination is computed by taking the arctangent of the Y component over the X component.

Fig. 13 plots declination in units of degrees versus time for each observatory over a two-day time period around June 1, 2013. The y-axis of the plots represents the declination as measured in degrees. Again, it is important to note that the declination values are not absolute, since they are computed from raw, uncorrected magnetometer data. The blue plot corresponds to the declination as measured at BRW. The red plot corresponds to the declination as measured at DED. The green plot corresponds to the declination as measured at CMO. The vertical scale of the y-axis for all three plots is 4°.

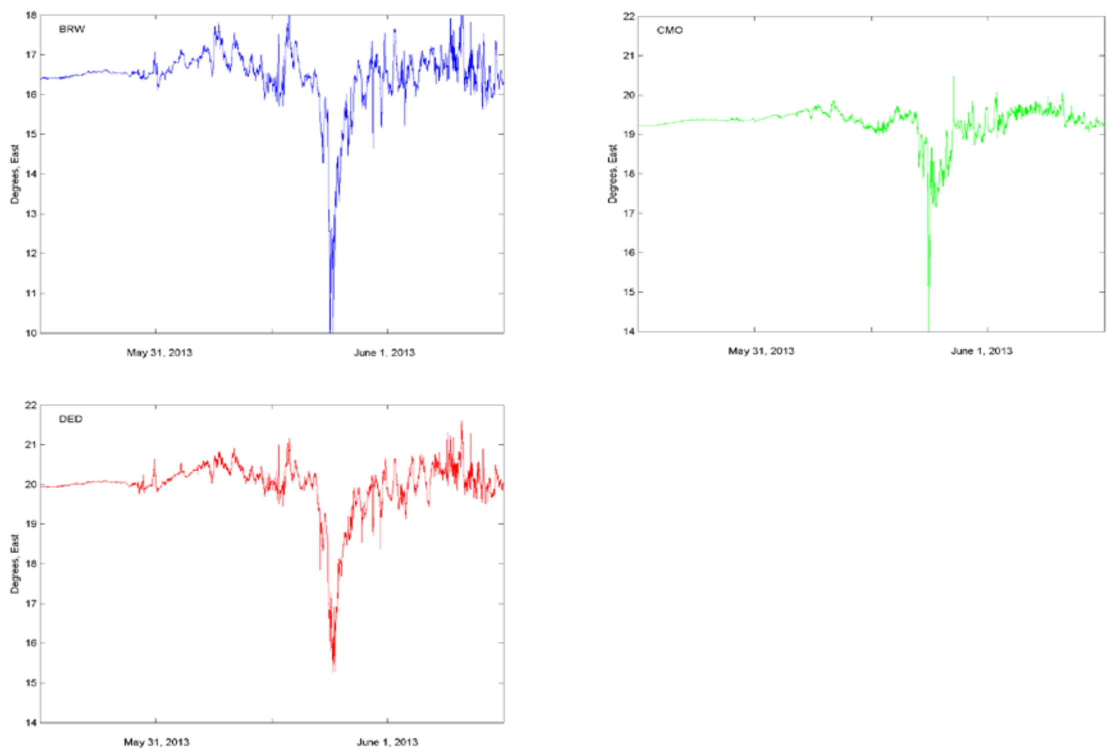

Fig. 13—The change in the declination as measured in BRW (blue), CMO (green) and DED (red) for May 31 - June 1, 2013

As one can see from **Fig. 13**, there is significant difference in the declination measured during the 48 hour period of the storm over the small geographic separation of the three observatories. Relying solely on one data source could potentially result in significant errors in the declination correction of well over 2°. These plots also show significant differences between BRW and DED compared to CMO which is at a slightly lower latitude. But is this relationship always true? To answer this question, the authors examined the declination measured at BRW and CMO for the Halloween magnetic storm of 2003 **(Fig. 14)**. The sudden commencement of this storm has a nearly equal effect on the maximum amplitude of the delination deflection at the two observatories: about 600 minutes of arc, or about 10°. This demonstrates that the behavior of the magnetic field can vary significantly from one storm to the next. It is easy to see the importance of supplementing DED with data from BRW and CMO and when in doubt, it is better to measure the actual disturbance data than to rely solely on the models.

Applying Higher Frequency Observatory Data

Higher frequency magnetic field data are much more useful in describing and analyzing the disturbance fields, especially at high latitudes. In addition to one-minute data, the USGS also records one-second data from its observatories. The rate of change of the declination at the three observatories was determined by computing the first differences of the one-second declination values **(Fig. 15)**.

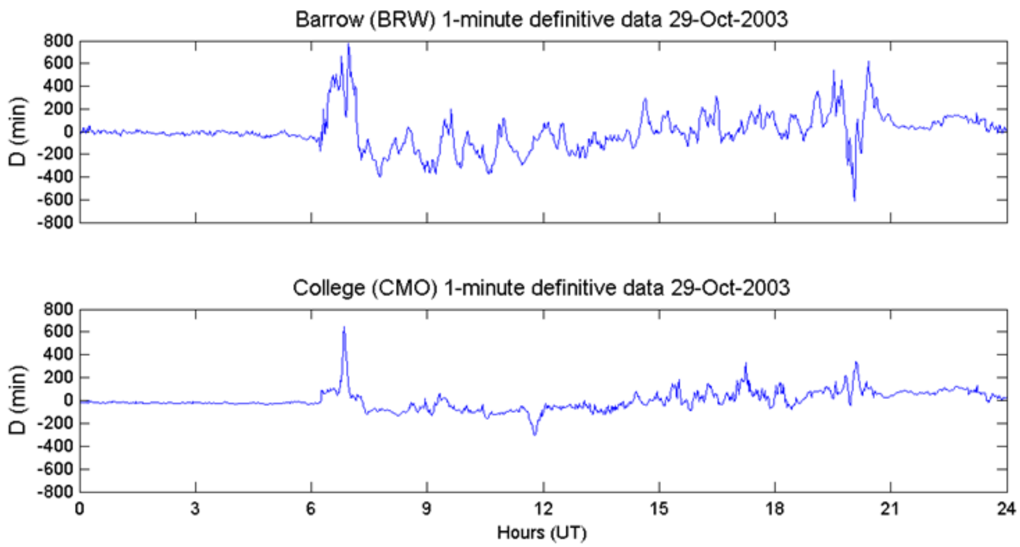

Fig. 14—The declination as measured in BRW (Top) and CMO (Bottom) for 24 hours on October 29, 2003.

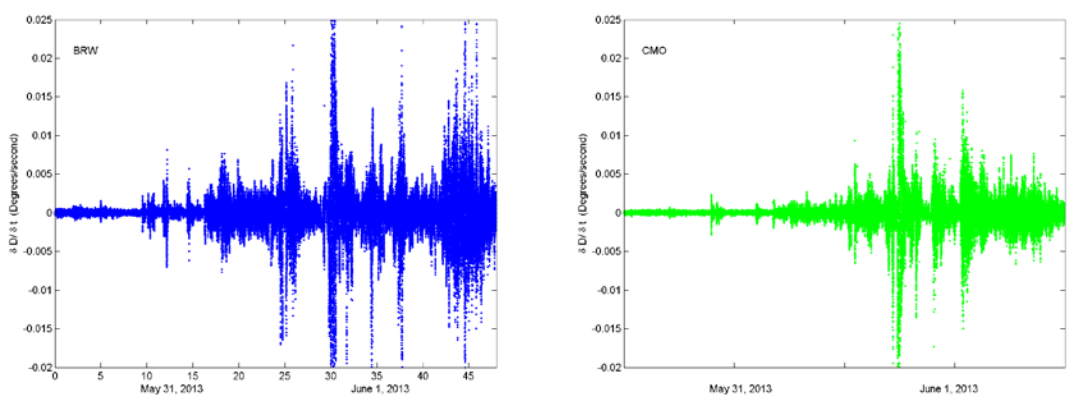

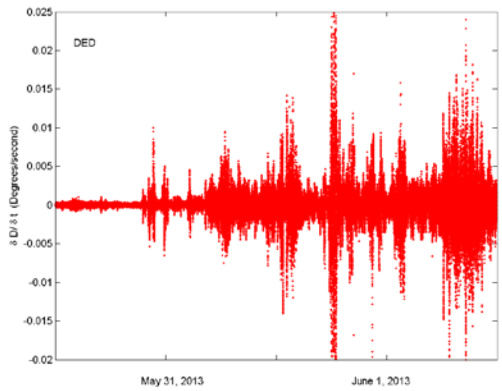

Fig. 15—The rate of change of declination as measured at BRW (blue), CMO (green), and DED (red) for May 31 - June 1, 2013

As shown in **Fig. 15**, the maximum change in declination exceeds 0.02°/second at all three sites. Rapid changes in the magnetic field can significantly impact the oil field operations in this area. It is also interesting to note that although the amplitude of change in declination at CMO is much smaller than that of BRW and DED, the rate of change at CMO is as great, if not greater, than BRW and DED during the sudden commencement. This further emphasizes the value of BRW, CMO, and DED as a supplement to the data collected and used by the oil industry on the North Slope of Alaska.

DED versus MWD Reading Comparisons

The plots below demonstrate the real-time implementation of geomagnetic referencing to improve the accuracy of MWD surveys. In **Fig. 16**, raw measurements of magnetic field strength and magnetic dip angle from the MWD tool's magnetometers are compared to the main field model, which is illustrated by the green lines. The red lines above and below the green reference value represent the limits of the field acceptance criteria (FAC) that are used as the first QA/QC measure to ensure adequate survey quality. Based on the erratic nature of these points and the instances when the FAC lines are crossed, it would be impossible in this instance to drill ahead with the assurance of good-quality surveys. Such erratic measurements could indicate MWD tool failure, external interference from nearby wellbores, magnetic mineral in the mud, magnetic sediments or other abnormalities.

In **Figs. 17—18**, the compared data are referenced against real-time measurements made at the DED rather than against the main field model. These plots clearly indicate that the measurements made by the MWD magnetometers in the borehole match the measurements made by the offsite DED magnetometers. This comparison shows that the erratic data is an actual tool measurement, which leads to high confidence in the MWD magnetometer readings. Cessation of drilling is not necessary. After geomagnetic reference processing, these surveys can be implemented with confidence.

In addition to providing assurance of the MWD tool's measurements, the correlation between the two sets of measurements also validates the data coming from the DED. In particular, the correlation of the magnetic field strength and dip angle indicates that the magnetic declination derived from the DED can be used in place of the declination provided by the less accurate main field model.

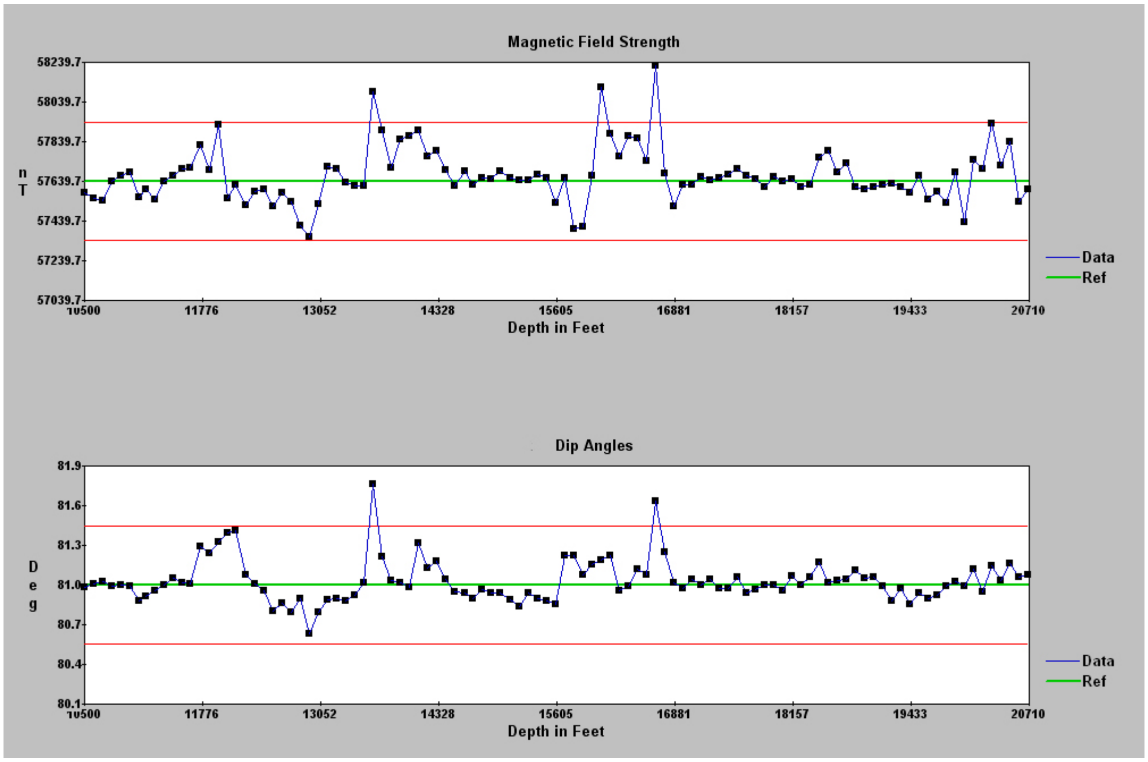

Fig. 16—MWD survey data (blue) referenced to the main field model (green) and acceptance lines (red).

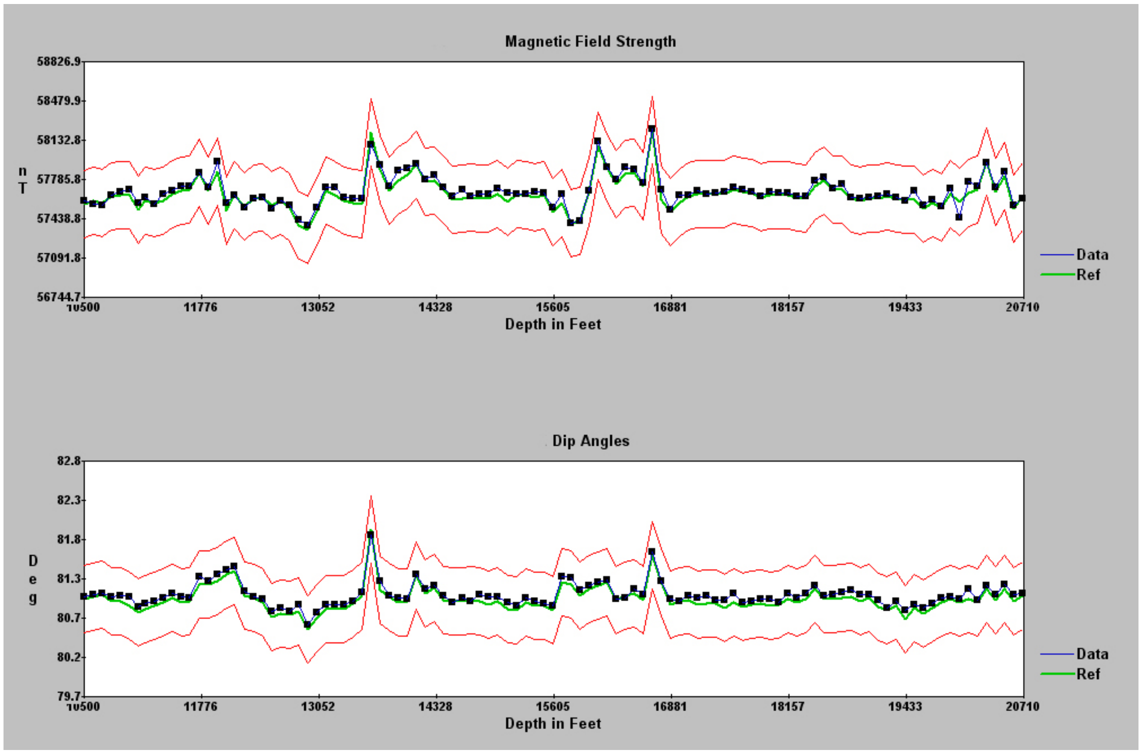

Fig. 17—Magnetic MWD survey data referenced to DED data (green) and acceptance lines (red).

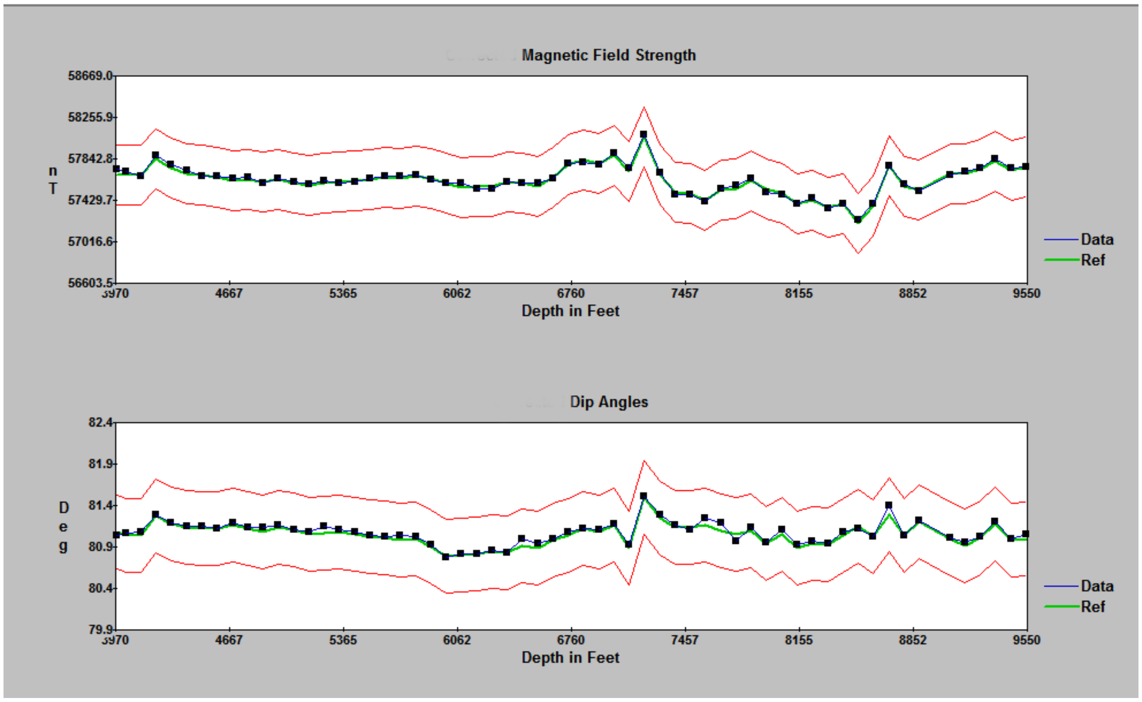

Fig. 18—Magnetic MWD survey data referenced to DED data (green) and acceptance lines (red).

Applications

Case History -Nikaitchuq Field Exploitation

The main reservoirs of the Nikaitchuq field are the OA and N sands within the Schrader Bluff formation **(Figs. 19 and 20).** The Schrader Bluff formation consists dominantly of marine sandstones and shale deposited within a foreland basin (Colville basin) during the late Cretaceous period. At that time, the source of the sediments was from the southwest, and toward this direction the Schrader Bluff interfingers with the nonmarine or marginal marine sediments of the Prince Creek formation. Toward the basin, far from the sediment source, the Schrader Bluff interfingers with the deeper marine shales of the Canning formation.

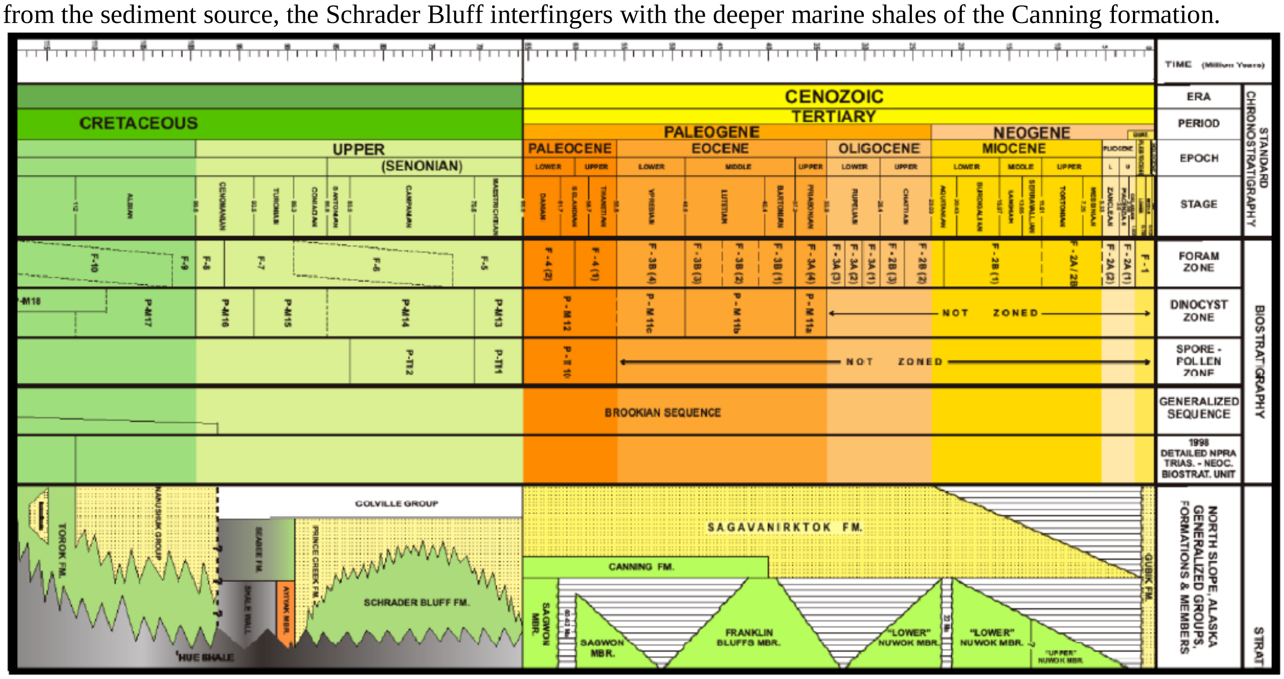

Fig. 19—Nikaitchuq geological sequence, source rock intervals and principle reservoirs

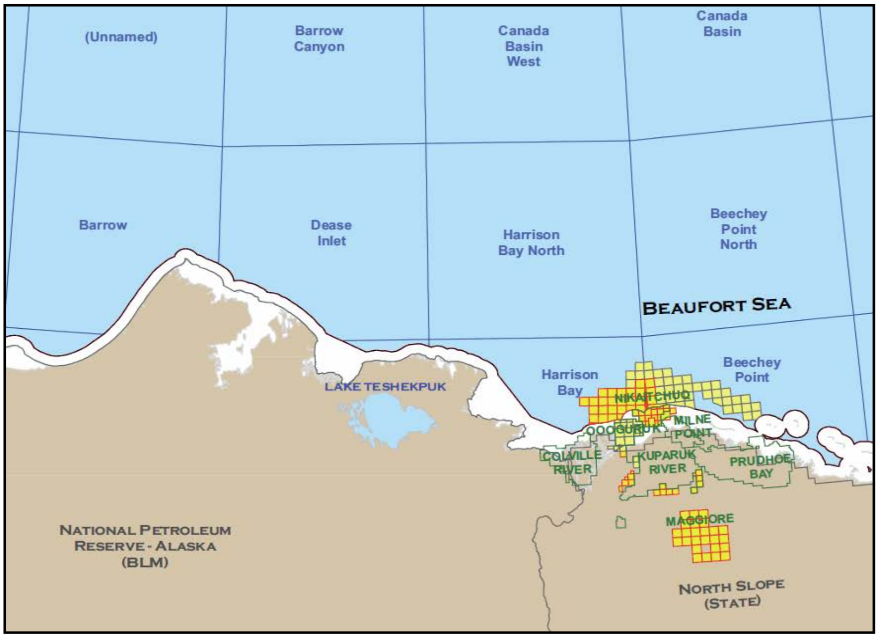

Fig. 20—The Nikaitchuq field and location (right) in the North Slope region of Alaska.

The structural setting of the reservoirs is a monocline, dipping very gently to the northeast. The trap mechanism is structural and stratigraphic. Several "updip" wellbores located south and west from the main Nikaitchuq area record a thin oil-bearing sand or no sand at all at the OA stratigraphic level. The OA field oil/water contact has been detected by log analysis at 4,177 ft true vertical depth subsea (TVDSS) in well Nikaitchuq 2. The continuity of the structure is interrupted, for the most part, by a set of northwest/southeast normal faults associated to the early Cretaceous rifting of the Beaufort Sea. A minor concurrent set of faults, striking northeast/southwest, is also present. Because of the thin development of the OA sand, the presence of continuous faults with throws greater than 30 to 40 ft could represent a tight barrier. Several pieces of evidence lead to a common conclusion that a major compartmentalization is occurring between the Kigun/Tuvaaq and OP-I2 "updip" portion of the field and the "downdip" area delineated by the Nikaitchuq wellbores and OP-I1. Within the two regions, oils with different qualities and properties have been sampled.

The development of the Nikaitchuq field involved two primary surface locations: the coastal Oliktok Point drilling pad and the Spy Island drilling pad off the coast. The drilling program was based on alternating producer and injector wells. The long lateral production/injection intervals of the wells would be drilled in parallel to one another with an approximate spacing of 1200 ft between each producer and injector. This spacing was selected to optimize production from the target reservoirs. Faulting was also taken into consideration during the well planning phase.

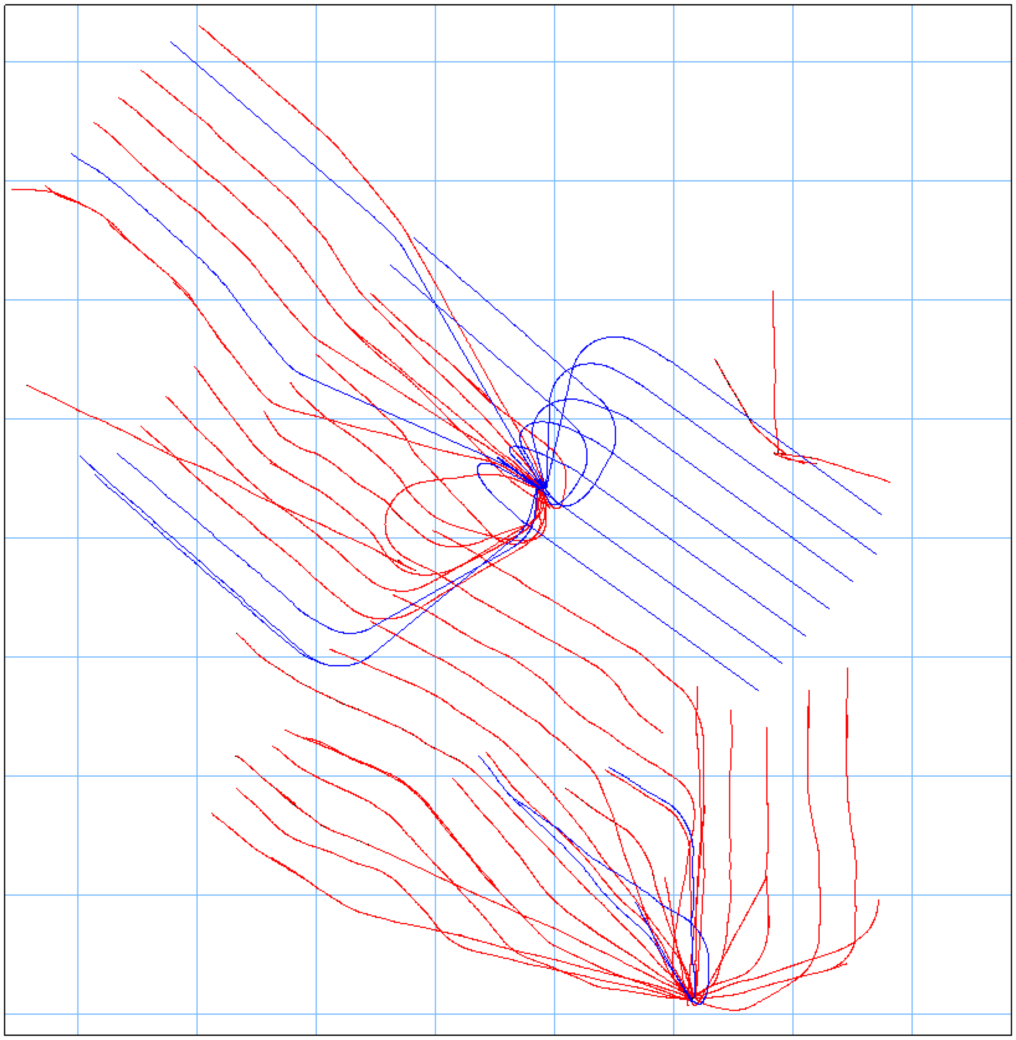

Fig. 21—The Nikaitchuq field spider plot in the North Slope region of Alaska. Existing wellbores (red) and the planned wellbores (blue).

Due to the extended well lengths and the subsurface wellbore density, minimizing anti-collision risks is a significant challenge. As the depth of each well extends farther, the uncertainty accumulates and, if unaddressed, can lead to a significant probability of collision **(Fig. 21).** By incorporating the DED geomagnetic observatory and North Slope geomagnetic reference model, the challenging well placement and anti-collision objectives of the Nikaitchuq objectives have been met.

Beyond MWD: Applications of Magnetic Observatories for Space Weather

As described earlier in this report, high latitude observatories such as DED can provide critical real-time data for accurate positioning while drilling (MWD) is in progress. However, data from ground-based magnetic observatories also play an important role in the diagnosis of space weather conditions, which in turn are critical to a modern, technologically-based society. Large magnetic storms, as shown in **Fig. 22**, can cause loss of radio communications, reduce the accuracy of global positioning systems, damage satellite electronics, increase pipeline corrosion, and induce voltage surges in electric power grids, causing blackouts. (Love and Finn, 2011).

Ground-based magnetic observatories are useful for a wide variety of space weather projects. For example, detailed ground-space analyses can be performed utilizing 1-second observatory data coupled with magnetic field data from low-Earth-orbiting satellites such as CHAMP and SWARM (Matzka et. al., 2010). The data from many high latitude observatories are also used to compute the auroral electrojet index (AE), which is a global measure of high latitude disturbance due to enhancements of the auroral electrojet. K values derived from USGS observatories in Boulder, CO, Fredericksburg, VA, and Fairbanks are the basis for NOAA Space Weather Prediction Center's issuance of geomagnetic storm alerts (http://www.swpc.noaa.gov). The K index is a characterization of local disturbance on a 0 to 9 scale, with values 0 to 3, 4 to 6, and 7 to 9 considered low, moderate, and high disturbance levels, respectively. The USGS recently began development of real-time K and AE indices, as part of a larger effort within the space weather community for developing a coordinated, operational network for monitoring and modeling space weather.

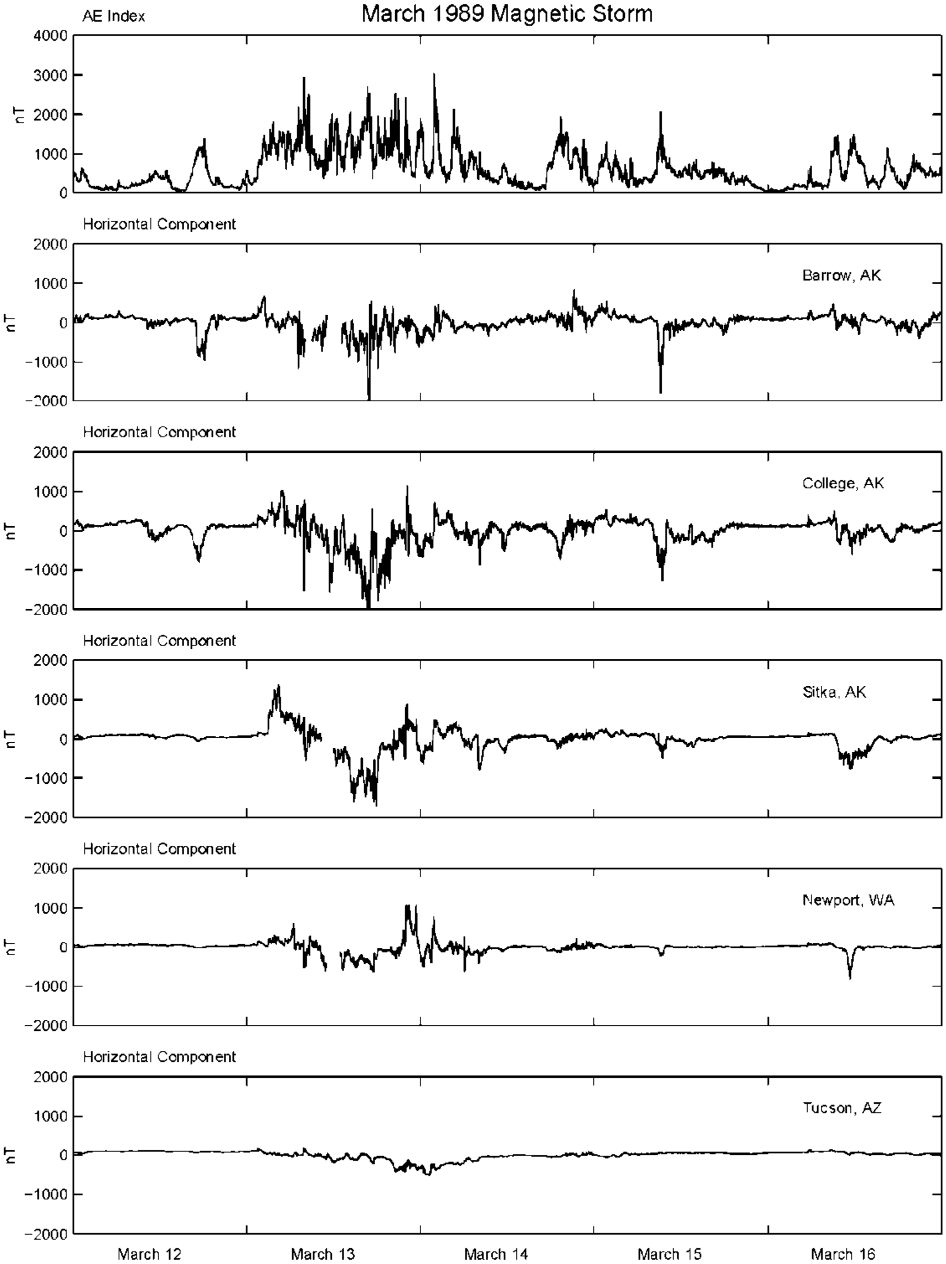

Fig. 22 — Measurements made during the “great storm” of March 1989. The top panel is the AE index, which measures auroral electrojet current; below are the horizontal magnetic fields as measured at five different USGS magnetic observatories.

Geomagnetic pulsations, with periods of seconds to a few minutes, are observed during substorm onset. This has motivated the development of related space weather monitoring indices derived from 1-second observatory data (Nose et. al. 1998). In addition to being a widely studied phenomenon in space weather (e.g. Elkington et al 1999; Hudson et al. 2000, 2004) , ultra-low frequency (ULF) geomagnetic pulsations are sometimes considered a source of noise in geophysical analysis techniques, such as aeromagnetic surveys (Wanliss and Antoine, 1995) and transient electromagnetics. USGS is developing indices based on observed magnetic spectral intensity within defined frequency bands (Pc3, Pc4, and Pc5) for use as a real-time monitor of geomagnetic fluctuations at USGS magnetic observatory locations (Xu et al., 2013). When presented geographically, these can be used asan initial step for spatial analysis of geomagnetic disturbance patterns.

Magnetic data from high-latitude observatories have additional applications beyond those for space weather and directional drilling. Geophysical investigations at high latitudes can be more complex than elsewhere in the world; the high levels of magnetic activity can make the interpretation of magnetic surveys more difficult. In Magnetotelluric (MT) studies at high latitudes, observatory data are used to model the magnetic field when the magnetic field deviates from the plane wave approximation used in MT. And finally, while most navigation is now done by GPS, compasses are still required equipment in aircraft. At high latitudes the magnetic declination changes more rapidly, up to 0.3° per year, than it does at lower latitudes, 0.05° per year. Magnetic observatories provide the necessary data to track the changes to keep navigational charts and airplane compasses up to date.

Conclusions

While MWD tools provide the most efficient method of wellbore surveying, error sources associated with the magnetic component of MWD surveys pose a major obstruction to their implementation on high-latitude projects with stringent well placement needs. Complex reservoir developments require surveying precision to achieve HSE and subsurface goals. Between the increased impact of drillstring magnetic interference, the escalated level of solar activity and the unmodeled crustal anomalies, standard MWD surveying practices are insufficient in addressing the needs of the most demanding operations. By implementing advanced geomagnetic referencing techniques, the critical error sources associated with geomagnetic field can be eliminated. In doing so, MWD surveys with geomagnetic referencing offer both operational efficiency and superior accuracy, providing Arctic operations with an extremely valuable tool.

The value of geomagnetic referencing has been clearly demonstrated on Eni Petroleum's Nikaitchuq project. This complex, extended-reach drilling campaign at extreme northern latitude has created new challenges for wellbore surveying. By implementing advanced geomagnetic referencing processing and using superior-quality data from the DED magnetic observatory, the challenges of drilling wellbores with a high degree of difficulty in adverse magnetic conditions can be addressed in real time. Drilling activities can proceed without the need for dedicated surveying operations beyond time-efficient MWD survey stations. The DED observatory and geomagnetic referencing techniques serve as critical enablers by ensuring the delivery of geological objectives and minimizing collision risks through enhanced surveying accuracy, all without any cessation in drilling activity. High-latitude observatories such as BRW and CMO, near DED, can also be used to augment data obtained through MWD surveys and regional models. Magnetic observatories such as DED have also demonstrated their value in a wide variety of scientific applications including those related to monitoring space weather phenomena.

Moving forward, the techniques applied on the Nikaitchuq project in Alaska can serve as a blueprint for overcoming wellbore positioning obstacles across the Arctic and in other magnetically challenging environments. The ability to provide accurate wellbore surveys while maximizing efficiency will prove vital as geological targets become smaller and the search for new resources pushes the industry farther and farther north.

Acknowledgments

The authors appreciate the permission of Eni Petroleum, the USGS, MagVAR and Schlumberger for their permission to publish the material contained in this paper. We thank them for their contributions and for ensuring that the operations were safely and successfully executed. We thank J. L. Gannon, C. Skokan, and J. J. Love for reviewing a draft manuscript.

References

Elkington, Scot R., Mary K. Hudson, and Anthony A. Chan. "Acceleration of relativistic electrons via drift-resonant interaction with toroidal-mode Pc-5 ULF oscillations." *Geophysical research letters* 26.21 (1999): 3273-3276.

Gannon, J. L., “Superposed epoch analysis and storm statistics from 25 years of the global geomagnetic disturbance index, USGS-Dst”, *USGS Open File Report 2012-1167* (2012), 15p.

Hudson, M. K., et al. "Increase in relativistic electron flux in the inner magnetosphere: ULF wave mode structure." *Advances in Space Research* 25.12 (2000): 2327-2337.

Hudson, M. K., et al. "A study of Pc-5 ULF oscillations." *Annales Geophysicae*. Vol. 22. No. 1. 2004.

Kerridge, David, Intermagnet: Worldwide Near-Real-Time Geomagnetic Observatory Data, British Geological Survey, 2001. (http://www.intermagnet.org/publications/IM_ESTEC.pdf)

Love, J. J. & Finn, C. A., 2011. The USGS Geomagnetism Program and its role in space weather monitoring, *Space Weather*, 9, S07001, doi:10.1029/2011SW000684.

Matzka, J., A. Chulliat, M. Mandea, C. Finlay, and E. Qamili, 2010, Geomagnetic Observations for Main Field Studies: From Ground to Space, *Space Sci. Rev.*, 155, 29-64, doi: 10.1007/s11214-010-9693-4.

Nose, M., T.Iyemori, M. Takeda, T. Kamei, D. K. Milling, D. Orr, H. J. Singer, E. W. Worthington, and N. Sumitomo, 1998, Automated detection of Pi 2 pulsations using wavelet analysis: 1. Method and an application for substorm monitoring, *Earth Planets Space*, 50, 773-783.

St.-Louis, Benoit, editor, Intermagnet Technical Reference Manual, Version 4.5, 2011 (http://www.intermagnet.org/publications/im_manual.pdf)

Wanliss, J.A., and Antoine, L.A.G., 1995, Geomagnetic micropulsations—Implications for high resolution aeromagnetic surveys: *Exploration Geophysics*, v. 26, p. 535–538.

Worthington, E. W. & Love, J. J., 2002. Geomagnetic field monitoring at Barrow, Alaska, Climate Monitoring and Diagnostics Laboratory, NOAA, US Dept. Commerce, 26, 166-170.

Xu, Z., J.L. Gannon and E.J. Rigler, “Report of Geomagnetic Pulsation Indices for Space Weather Applications”, *USGS Open-File Report*, in press, (2013),